

A Multifrequency HYSCORE Study of Weakly Coupled Nuclei in Frozen Solutions of High-Spin Aquometmyoglobin

Inés García-Rubio,^{*,†} Maria Fittipaldi,^{‡,§} Florin Trandafir,[‡] and Sabine Van Doorslaer^{*,‡}

Laboratory of Physical Chemistry, ETH Zurich, CH-8093 Zürich, Switzerland, and Department of Physics, University of Antwerp, B-2610 Wilrijk-Antwerp, Belgium

Received September 2, 2008

In this work, we show the extreme power of multifrequency HYSCORE (hyperfine sublevel correlation spectroscopy) techniques to unravel the hyperfine interactions of the electron spin with the remote nuclei in the heme site of high-spin ferric heme proteins. Horse heart aquo-metmyoglobin was used as a model system to demonstrate the power of these techniques. Experimental evidence was collected and assigned to protons of the proximal histidine ligand, to the mesoprottons of the heme ligand, and to two different protons of the distal water ligand. The latter difference relates to the stabilization of the water ligand by the E7His residue. Furthermore, HYSCORE signals of the remote N_δ of the proximal (F8) and N_ε of the distal (E7) histidine were detected. Finally, correlation peaks from the lesser-abundant ¹³C nuclei of the heme ligand could be detected. These novel results allow dissection of the hyperfine couplings into individual contributions and calculation of the spin density in the π and σ orbitals, thus completing earlier electron paramagnetic resonance and liquid-state NMR data.

Introduction

Heme proteins are ubiquitous among living organisms, where they execute a great variety of tasks such as transport, detoxification, electron transport, protection against oxidation, and so forth. All of these proteins share the same cofactor, an iron–porphyrin group called heme, which plays a central role in their function and determines many of the protein's physicochemical properties. Consequently, studying the electronic and geometric structure of the heme pocket can give key information about reaction mechanisms of these proteins.

One of the several functional states of heme proteins involves a ferric heme iron, Fe³⁺ (d⁵), in a high-spin (HS) configuration, $S = 5/2$. Because of the paramagnetic nature of this state, electron paramagnetic resonance (EPR) techniques provide excellent characterization tools for this system.^{1,2} Since the standard continuous-wave EPR spectra

reveal little information on the iron site, other than its spin state, more advanced techniques need to be applied to determine the hyperfine interactions between the electron spin and the nuclear spins present in the surroundings of the metal. Traditionally, these interactions are probed using electron nuclear double resonance (ENDOR)^{3–7} or paramagnetic NMR,^{2,8–11} depending on the nuclei that are targeted.

ENDOR has yielded very detailed information about the directly coordinated nitrogens of the porphyrin ring in HS heme proteins,^{3–7} but in most cases, the full set of magnetic parameters could only be derived from single-crystal ENDOR studies.⁵

* Authors to whom correspondence should be addressed. E-mail: sabine.vandoorslaer@ua.ac.be (S.V.D.), garciarubio@phys.chem.ethz.ch (I.G.-R.).

† ETH Zurich.

‡ University of Antwerp.

§ Current address: INSTM - Department of Chemistry, University of Florence, Via della Lastruccia 3, I-50019 Sesto Fiorentino, Italy.

(1) Palmer, G. *Electron Paramagnetic Resonance of Hemoproteins*. In *Iron Porphyrins*; Addison-Wesley: London, 1983; Vol. II.

(2) Walker, F. A. *Inorg. Chem.* **2003**, *42*, 4526.

(3) Feher, G.; Isaacson, R. A.; Scholes, C. P.; Nagel, R. *Ann. N.Y. Acad. Sci.* **1973**, *222*, 86.

(4) Mulks, C. F.; Scholes, C. P.; Dickinson, L. C.; Lapidot, A. *J. Am. Chem. Soc.* **1979**, *101*, 1645.

(5) Van Camp, H. L.; Scholes, C. P.; Mulks, C. F. *J. Am. Chem. Soc.* **1976**, *98*, 4094.

(6) Van Camp, H. L.; Scholes, C. P.; Mulks, C. F.; Caughey, W. S. *J. Am. Chem. Soc.* **1977**, *99*, 8283.

(7) Scholes, C. P.; Lapidot, A.; Mascarenhas, R.; Inubushi, T.; Isaacson, R. A.; Feher, G. *J. Am. Chem. Soc.* **1982**, *2724*.

(8) Krishnamoorti, R.; La Mar, G. N.; Mizukami, H.; Romero, A. *J. Biol. Chem.* **1984**, *259*, 265.

(9) La Mar, G. N.; Budd, D. L.; Smith, K. M.; Langry, K. C. *J. Am. Chem. Soc.* **1980**, *102*, 1822.

(10) Rajarathnam, K.; La Mar, G. N.; Chiu, M. L.; Sligar, S. G.; Singh, J. P.; Smith, K. M. *J. Am. Chem. Soc.* **1991**, *113*, 7886.

(11) Shokhireva, T. K.; Smith, K. M.; Berry, R. E.; Shokhirev, N. V.; Balfour, C. A.; Zhang, H.; Walker, F. A. *Inorg. Chem.* **2007**, *46*, 170.

Information on the hyperfine interactions of the more remote nuclei is generally obtained from NMR studies.^{2,8–11} When there is a paramagnetic entity near a nuclear spin, its corresponding NMR peak is shifted due to the interaction of the nucleus with the electronic magnetic moment (paramagnetic shift). In the NMR studies of ferric HS heme proteins, the fact that the contact shift can be related to the isotropic hyperfine interaction (A_{iso}) is exploited to study the magnitude and the sign of the spin density at the protons and the carbons in the porphyrin ring.^{9,12} The ^{13}C contact shifts in ^{13}C -porphyrin-labeled HS heme proteins have been correlated with structural properties of the proteins, like the coordination number of the metal.¹³ Note that the NMR approach is restricted to the analysis of the remote nuclei, because the large hyperfine interaction of the directly coordinated nuclei broadens the NMR lines beyond detection.

For most cases, a combination of the NMR and ENDOR studies will still provide only partial information. The NMR analysis reveals only information about the A_{iso} values of the remote nuclei, failing to reveal the anisotropic part of their hyperfine tensor. In principle, the ENDOR analysis can provide this information, but spin-system-specific problems hamper this in practice (see refs 14 and 15 for a detailed discussion).

Lately, the great potential of the high-resolution pulse EPR techniques to study HS ferric heme proteins has just begun to be exploited.^{15–17} We have proven the extremely high performance of these methods to characterize the *first coordination sphere* of the heme iron in frozen solutions of aquometmyoglobin (aquometMb), extracting information that could previously only be obtained from a single-crystal study.¹⁴ Here, we prove that multifrequency HYSCORE (hyperfine sublevel correlation) experiments allow for a detailed analysis of different *remote magnetic nuclei*, revealing new information about their magnetic parameters. Using X- and Q-band HYSCORE, the hyperfine interactions with the mesoprotons of the porphyrin ring, the protons attached to C_ϵ and C_δ of the proximal histidine, the two different protons from the axial water, the N_δ nucleus of the proximal histidine, and the N_ϵ nucleus of a distal histidine could be determined (Figure 1). Moreover, we were able to detect the hyperfine interactions with the carbons of the porphyrin ring (α - and β -pyrrole and mesocarbons) without the need for isotope labeling.

Experimental Section

Sample Preparation. The lyophilized horse heart metmyoglobin was purchased from Sigma Co. The protein was solubilized in 50 mM phosphate buffer, pH 7, and used without further purification.

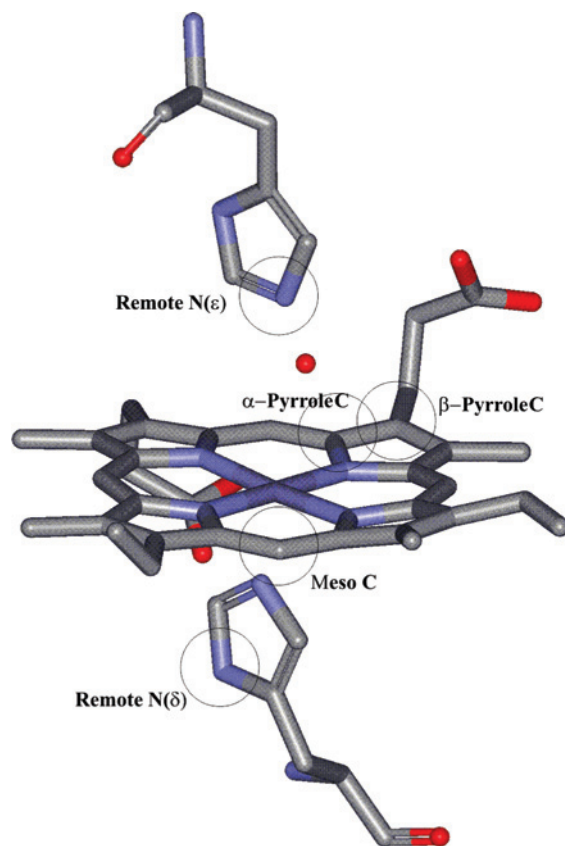


Figure 1. Structure of the active site of aquometmyoglobin. The magnetic nuclei of interest have been highlighted.

To obtain a good quality glass upon freezing the sample, 30% glycerol was added to the protein solution. The sample was then transferred to clear fused quartz tubes and kept at liquid nitrogen temperatures until used. H/D exchange was obtained by dissolving the protein in a buffer based on D_2O and deuterated glycerol (both 99.9% isotope enrichment, from Cambridge Isotope Laboratories, Inc.).

EPR Spectroscopy. X-band pulse EPR measurements were carried out at 3.8 K on a Bruker E580 (ETH Zurich) and a Bruker ESP380E (University of Antwerp) spectrometer, both operating at ~ 9.7 GHz and equipped with helium continuous-flow cryostats from Oxford, Inc. A similar cryostat was used in combination with a home-built hybrid EPR spectrometer¹⁸ working at a microwave frequency of 35 GHz (Q-band). The Q-band pulse EPR experiments were done at 5.5 K. For these experiments, a homemade loop-gap resonator yielding a very high B_1 field at the sample position was used.¹⁹ All of the measurements were performed at the highest repetition rate (3.3 kHz) achievable with the experimental equipment.

HYSCORE^{20,21} is a pulse EPR experiment that correlates nuclear frequencies in one electron spin manifold to nuclear frequencies in the other electron spin manifold. The pulse sequence $\pi/2-\tau-\pi/2-t_1-\pi-t_2-\pi/2-\tau$ -echo was used, together with an eight-step phase cycle to remove unwanted echoes. The pulse lengths were, unless stated otherwise, $t_\pi = 16$ ns and $t_{\pi/2} = 24$ ns; t_1 and t_2 had initial values of 96 ns and were varied in steps of 16 ns (or 8 ns).

- (12) Alontaga, A. Y.; Bunce, R. A.; Wilks, A.; Rivera, M. *Inorg. Chem.* **2006**, *45*, 8876.
- (13) Cheng, R.-J.; Chen, P.-Y.; Lovell, T.; Liu, T.; Noodleman, L.; Case, D. A. *J. Am. Chem. Soc.* **2003**, *125*, 6774.
- (14) Fittipaldi, M.; Garcia-Rubio, I.; Trandafir, F.; Gromov, I.; Schweiger, A.; Bouwen, A.; Van Doorslaer, S. *J. Phys. Chem. B* **2008**, *112*, 3859.
- (15) Trandafir, F.; Heerd, P.; Fittipaldi, M.; Vinck, E.; Dewilde, S.; Moens, L.; Van Doorslaer, S. *Appl. Magn. Reson.* **2007**, *31*, 553.
- (16) Garcia-Rubio, I.; Braun, M.; Gromov, I.; Thony-Meyer, L.; Schweiger, A. *Biophys. J.* **2007**, *92*, 1361.
- (17) Smirnova, T. I.; Davis, M. F.; Franzen, S. *J. Am. Chem. Soc.* **2008**, *130*, 2128.

(18) Gromov, I.; Shane, J.; Forrer, J.; Rakhmatoullin, R.; Rozentzwaig, Y.; Schweiger, A. *J. Magn. Reson.* **2001**, *149*, 196.

(19) Forrer, J.; García-Rubio, I.; Schuhmann, R.; Tschaggelar, R.; Harmer, J. *J. Magn. Reson.* **2008**, *190*, 280.

(20) Höfer, P. *J. Magn. Reson., Ser. A* **1994**, *111*, 77.

(21) Schweiger, A.; Jeschke, G. *Principles of Pulse Electron Paramagnetic Resonance*; Oxford University Press: Oxford, U.K., 2001; p 289.

Spectra were taken at different values of τ to minimize the effect of the blind spots. The sensitivity of the Q-band HYSOCORE experiments was improved using the SMART HYSOCORE sequence^{21,22} $p_M - t_1 - \pi - t_2 - p_M - \tau - \pi - \tau - echo$. Here, the first and third matched pulses (p_M) had a length of 32 ns and a field strength ν_1 of 31 MHz. A four-step phase cycle was used to eliminate unwanted echoes.

The time traces were baseline-corrected, windowed, and zero-filled. Subsequently, a 2D Fourier transform was performed, and the absolute value of the spectrum was calculated.

Theoretical Basis. The Spin Hamiltonian. The spin Hamiltonian for a spin system with an Fe(III) ion in the HS state (electronic configuration $3d^5$, $S = 5/2$) interacting with m nuclear spins, I_i , is given by the following equation:

$$H = \frac{\mu_B \vec{B}_0 \vec{g}_e \vec{S}}{h} + \vec{S} \vec{D} \vec{S} + \sum_i^m \vec{S} \vec{A}_i \vec{I}_i - \frac{\mu_n}{h} \sum_i^m g_n \vec{B}_0 \vec{I}_i + \sum_{I_i > 1/2} \vec{I}_i \vec{Q}_i \vec{I}_i \quad (1)$$

Hereby, we make use of the arrows to indicate vectors and the \hat{x} to denote matrices. μ_B and μ_n are the Bohr and nuclear magneton, respectively, and B_0 is the static magnetic field. The first term describes the electron Zeeman interaction, which in the case of metmyoglobin is nearly isotropic with $g \approx g_e$.^{23,24} The second term represents the zero-field splitting (ZFS). The third term takes into account the hyperfine interactions with magnetic nuclei in the active site. Each hyperfine interaction can be written as the sum of an isotropic part (A_{iso}) and an anisotropic contribution. If the interacting nucleus is located more than 0.25 nm away from the metal center²¹ and there is no significant spin delocalization, the point-dipolar approximation can be used to calculate the latter contribution:

$$H = A_{iso} \vec{S} \vec{I} + \vec{S} \vec{T} \vec{I} \quad (2)$$

whereby A_{iso} is directly related to the spin density at the nucleus, $|\Psi_0(0)|^2$, and the matrix \hat{T} has the following mathematical expression:

$$\hat{T} = \frac{\mu_0}{4\pi h} g_e \mu_B g_n \mu_N \frac{(3\vec{u}' \cdot \vec{u} - 1)}{r^3} f \quad (3)$$

where \vec{u} is here the unit vector representing the direction joining the electron and the nucleus and r is the distance between them. f denotes the fraction of spin density at the central metal atom.

The fourth term in eq 1 accounts for the nuclear Zeeman interaction, which is isotropic, and the fifth for the nuclear quadrupole interactions of nuclei with a spin larger than 1/2. The nuclear quadrupole principal values, $[Q_x, Q_y, Q_z]$, of the traceless \hat{Q} tensor are sometimes expressed as $[-K(1 - \eta), -K(1 + \eta), 2K]$ with the quadrupole coupling constant $K = e^2 q Q / 4I(2I - 1)h$ and the asymmetry parameter $\eta = (Q_x - Q_y) / Q_z$. Q is the nuclear quadrupole moment and eq is the electric field gradient.

Effective g and Hyperfine Values. In the case of aquometMb, the ZFS is dominating the spin Hamiltonian ($D = 9.26 \text{ cm}^{-1}$),²⁵ and at X- and Q-band microwave frequencies, the EPR transitions occur within the ground doublet ($\pm 1/2$). Hence, the system can be described as an effective spin $S_{\text{eff}} = 1/2$ system with effective

magnetic parameters that deviate from the ones defined in eq 1 in the following way:^{7,14}

$$g_x^{\text{eff}} \approx 3g_x; \quad g_y^{\text{eff}} \approx 3g_y; \quad g_z^{\text{eff}} \approx g_z \quad (4)$$

$$A_{i,x}^{\text{eff}} \approx 3A_{i,x}; \quad A_{i,y}^{\text{eff}} \approx 3A_{i,y}; \quad A_{i,z}^{\text{eff}} \approx A_{i,z} \quad (5)$$

and

$$g_{n,i,x}^{\text{eff}} = g_n + \frac{2g_x \beta_e A_{i,x}}{\beta_n D}; \quad g_{n,i,y}^{\text{eff}} = g_n + \frac{2g_y \beta_e A_{i,y}}{\beta_n D}; \quad g_{n,i,z}^{\text{eff}} = g_n \quad (6)$$

Simulations of HYSOCORE Spectra. To calculate the full HYSOCORE patterns shown in the figures, we used EasySpin, a Matlab toolbox specially targeted at EPR simulations²⁶ (free download at www.easyspin.org). First, the orientation selection of the experiment was calculated; then, the nuclear frequencies were computed for the excited orientations using the high-spin Hamiltonian of eq 1.

Comparing EPR and NMR Results. In the following sections, we will compare the hyperfine interactions obtained from the HYSOCORE experiments with previous measurements of hyperfine interactions by NMR in protein solutions at room temperature. In the NMR literature, the chemical shift is given in units of parts per million. To relate these shifts to the hyperfine values, we assumed the diamagnetic shift of the nuclei to be negligible in comparison with the paramagnetic shift. We calculated the pseudo contact contribution to the paramagnetic shift with eq 45 in ref 27 using the structural data of the protein and a value of $D = 9.26 \text{ cm}^{-1}$. We found that this contribution was much smaller than the reported chemical shifts. Therefore, we interpreted the chemical shifts as being paramagnetic contact shifts and translated them to the isotropic hyperfine parameters using the following expression:^{2,27}

$$A_{iso} [\text{MHz}] = -\delta_{\text{con}} \frac{3\gamma_N kT}{2\pi g_e \beta S(S+1)} \quad (7)$$

Results

Figure 2 displays the X-band HYSOCORE spectrum of a frozen solution of aquometMb taken at a magnetic field value of 320 mT. Only the molecules for which the heme normal is approximately 10° away from the magnetic-field direction contribute to this spectrum. In the (+,+) quadrant, several correlation ridges due to different kinds of magnetic nuclei weakly coupled with the electron spin can be observed. In particular, a number of ridges appear in the region near the Larmor frequency of the protons (ν_H). In the low-frequency region of the spectrum, there are also several correlation peaks close to $2\nu_N$ and ν_C , which indicates that it is possible to detect some remote nitrogens and naturally abundant ^{13}C carbons in the active site.

Proton HYSOCORE Signals. In our previous studies of HS heme proteins,^{14–16,28} we already briefly discussed some proton signals detected in the X-band HYSOCORE spectra taken at an observer position corresponding to $g = g_n$. In particular, we focused on the water–proton cross peaks appearing at (17.9, 12) MHz in the HYSOCORE spectrum of aquometMb. These

(22) Jeschke, G.; Rakhmatullin, R.; Schweiger, A. *J. Magn. Reson.* **1998**, *131*, 261.

(23) Scholes, C. P.; Isaacson, R. A.; Feher, G. *Biochim. Biophys. Acta* **1972**, *263*, 448.

(24) Eisenberger, P.; Pershan, P. S. *J. Chem. Phys.* **1966**, *45*, 2832.

(25) Scholes, C. P.; Isaacson, R. A.; Feher, G. *Biochim. Biophys. Acta* **1971**, *244*, 206.

(26) Stoll, S.; Schweiger, A. *J. Magn. Reson.* **2006**, *42*.

(27) Kurland, R. J.; McGarvey, B. R. *J. Magn. Reson.* **1970**, *2*, 286.

(28) Ioanitescu, A. I.; van Doorslaer, S.; Dewilde, S.; Endewards, B.; Moens, L. *Mol. Phys.* **2007**, *105*, 2073.

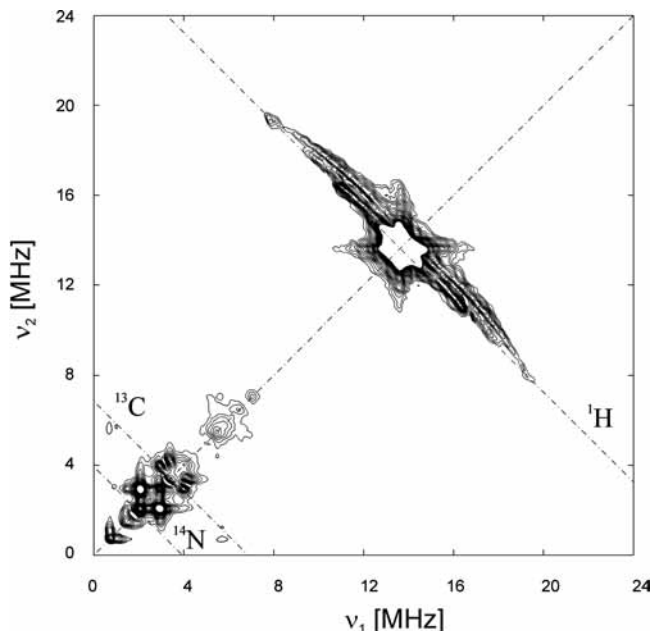


Figure 2. Standard X-band HYSCORE spectrum of a frozen solution of aquometmyoglobin near $g_{||}^{\text{eff}}$, $B = 320$ mT. This spectrum is the sum of two sets of data collected for $\tau = 80$ and 128 ns. The anti-diagonal lines cross the diagonal at the Larmor frequencies $2\nu_N$, ν_C , and ν_H . $T = 3.8$ K.

Table 1. Proton Structural and Hyperfine Coupling Parameters Used in the HYSCORE Simulations of Figures 3 and 4

	r (Fe–C) (Å)	θ (deg) ^a	ϕ (deg) ^a	T (MHz)	A_{iso} (MHz)	f
C_ϵ and C_δ (His)	3.26	± 40	0	2.0	+0.2	0.9
meso	4.45	90	45	0.9	+0.06	0.9
water (1)	2.70	20	165	4.1	-0.3	1
water (2)	2.80	16	45	3.6	+0.6	1

^a θ and ϕ are the polar angles that define the position of the vector r (Fe–H) with respect to the axes of the molecule.

cross peaks disappear upon deuteration of the solvent, whereby clear cross peaks appear at (2.7, 1.8) MHz, centered around the deuterium Zeeman frequency (see the Supporting Information). From these, the proton hyperfine coupling at this observer position can be estimated as ~ 5.9 MHz. The hyperfine coupling constant of this exchangeable proton is in agreement with the previously reported ENDOR studies^{3,4} and close to the one predicted for the protons of the coordinated water using the geometry given by the X-ray structures^{29–31} of aquometMb (note, $d(\text{O–H})$ is taken to be 0.1 nm), combined with the simple point-dipole approximation (eq 3). This suggests that the outer proton ridges in Figure 2 (spectrum taken 28 mT downfield from the $g = g_{||}^{\text{eff}}$ position) are also originating from the coordinated water molecule.

On going to lower fields, the signals of the weakly coupled nuclei fade away from the spectra, and at a field position corresponding to $g = g_{\perp}^{\text{eff}}$, the signals have disappeared both in the standard HYSCORE spectra and in the ENDOR spectra. Gaining information about the hyperfine coupling parameters for orientations different from $g_{||}^{\text{eff}}$ is, however, necessary in order to obtain a complete characterization of the proton hyperfine interactions.

Similarly as found for the HYSCORE cross peaks stemming from the coordinating nitrogens,¹⁴ the SMART-HYSCORE experiment proved to be useful in obtaining signals of protons at $g = g_{\perp}^{\text{eff}}$ (see Figure 3A). At this magnetic field, ν_H is 4.9 MHz. The appearance of correlation peaks in both quadrants of the HYSCORE spectrum suggests that some of the protons are nearing the cancellation condition ($|A^{\text{eff}}/2| \approx |\nu_H|$). However, the signal-to-noise ratio is not very good, most probably due to the fast electron spin relaxation at the given experimental conditions.

In order to increase the phase-memory time, T_m , the protein was prepared in deuterated water,³² and a series of SMART-HYSCORE experiments were performed at several values of the magnetic field ranging from the one corresponding to g_{\perp}^{eff} ($B_0 = 117$ mT) to 260 mT (Figure 4). A comparison of Figures 3A and 4 illustrates the improvements achieved by deuteration. The dots superimposed to the spectra in Figures 3 and 4 show the calculated nuclear frequencies for the spin system given in eq 1 interacting with the different protons in the heme pocket. The proton hyperfine interactions were assumed to be of the form given in eqs 2 and 3, that is, consisting of an isotropic contribution and a point-dipole anisotropic contribution. As starting values for the simulation procedure, the structural data from X-ray diffraction studies (with $d(\text{C–H}) = 0.1$ nm)^{29–31} and A_{iso} values from liquid NMR of aquometMb⁹ were used. This allowed the assignment of ridges to the respective protons. Once the ridges were assigned, the simulation parameters were changed so as to optimally fit the experimental data (Table 1, Figures 3 and 4). The HYSCORE ridges in Figure 4 could be assigned to the mesoprotons (green in the calculation) and to the protons attached to C_δ and C_ϵ of the directly coordinated histidine residue (red).

As expected for the SMART-HYSCORE experiment, the correlation patterns are not symmetric, and a number of combination peaks are also observed around twice the ν_H value.

In order to obtain more information on the protons of the water molecule that binds the Fe^{3+} ion at the distal side, we performed Q-band SMART-HYSCORE experiments at an observer position corresponding to $g = g_{\perp}^{\text{eff}}$ (Figure 3B). The spectrum displays well-defined correlation ridges around ν_H . The innermost ridge was assigned to mesoprotons based on the hyperfine parameters obtained from the X-band HYSCORE experiments. The outermost ridge, with its external borders at (14, 22) MHz, was assigned to the water protons, as it could be reproduced with the point-dipole hyperfine tensors calculated for the water protons. Furthermore, these ridges were found to disappear in the Q-band HYSCORE spectrum of aquometMb in deuterated water. In order to obtain a good agreement between the simulated and experimental nuclear frequencies, an isotropic hyperfine constant of -0.3 MHz has to be considered. It has to be underlined that good-quality Q-band SMART-HYSCORE spectra can be obtained at the $g = g_{\perp}^{\text{eff}}$ observer position

(29) Evans, S. V.; Brayer, G. D. *J. Mol. Biol.* **1990**, *213*, 885.

(30) Maurus, R.; Overall, C. M.; Bogumil, R.; Luo, Y.; Mauk, A. G.; Smith, M.; Brayer, G. D. *Biochim. Biophys. Acta* **1997**, *1341*, 1.

even without the use of a deuterated solvent, as we already reported previously.¹⁴

It is worth noting that in the standard X-band HYSCORE spectrum taken near $g_{\parallel}^{\text{eff}}$ (Figure 3C) as well as in the Q-band SMART HYSCORE spectrum at $g = g_{\perp}^{\text{eff}}$ (Figure 3B), an extra set of ridges can be distinguished at (10.5, 17.2) MHz (Figure 3C) and (14.8, 21.0) MHz (Figure 3B) that also disappear upon deuteration. The nuclear frequencies of this ridge can be reproduced if we consider a second water proton with slightly different hyperfine parameters (see Table 1). The structural

parameters of this proton are still compatible with crystallographic data. That means that we are most probably able to distinguish a small nonequivalence of the two water protons by the applied 2D-ESEEM techniques. An alternative explanation that cannot fully be ruled out is that two different conformations are frozen, which differ in the geometry of the water coordination in the heme pocket and hence give rise to two different water-proton HYSCORE signals.

The simulations of the HYSCORE peaks due to the water protons are given in Figure 3.

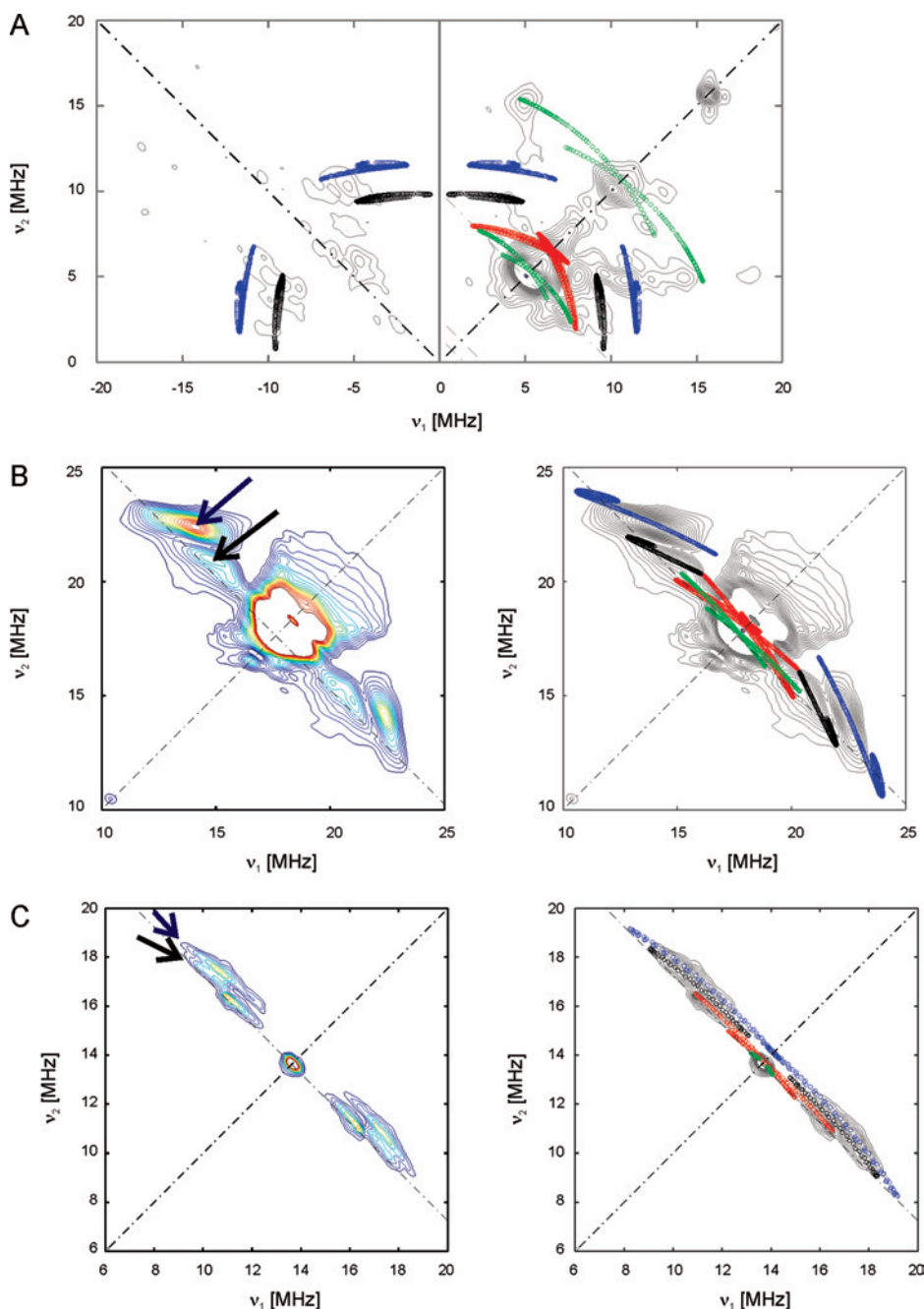


Figure 3. Proton HYSCORE spectra. (A) X-band SMART HYSCORE spectrum at $g = g_{\perp}^{\text{eff}}$, $B_0 = 117$ mT, $t(\text{pM}) = 32$ ns, $\tau = 120$ ns. (B) Q-band SMART HYSCORE spectrum at $g = g_{\perp}^{\text{eff}}$, $B_0 = 414$ mT, $t(\text{pM}) = 28$ ns. (C) Standard X-band HYSCORE spectrum near $g = g_{\parallel}^{\text{eff}}$, $B_0 = 320$ mT, $\tau = 128$ ns. The experimental spectra are shown alone on the left and together with the superimposed frequency calculations on the right. The circles display the calculated nuclear frequencies for the mesoproteins (green), ortho protons of the histidine ligand (bound to the C(δ) and C(ϵ) of the His (red), water protons 1 (blue), and water protons 2 (black) according to the parameters in Table 1. SMART HYSCORE spectra can display significant asymmetry. The spectra have not been symmetrized in order to get a better perception in distinguishing signals from noise. The dashed-dotted antidiagonal line in B and C crosses the proton Larmor frequency.

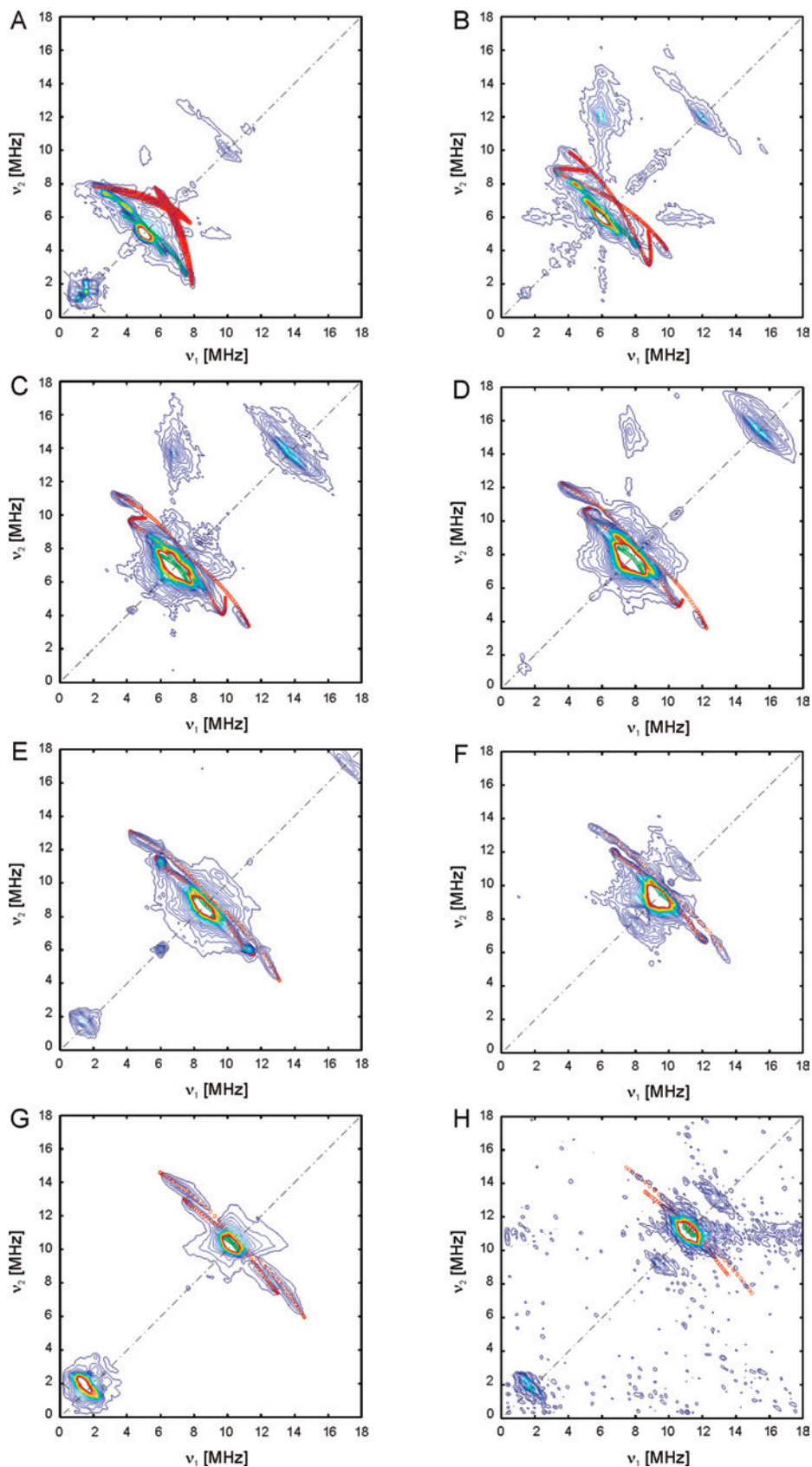


Figure 4. Proton X-band SMART-HYSCORE spectra of a frozen solution of deuterated aquometmyoglobin at (A) $B_0 = 117$ mT (g_{\perp}^{eff}), (B) $B_0 = 140$ mT, (C) $B_0 = 160$ mT, (D) $B_0 = 180$ mT, (E) $B_0 = 200$ mT, (F) $B_0 = 220$ mT, (G) $B_0 = 240$ mT, and (H) $B_0 = 260$ mT. The circles correspond to the calculated frequencies of the mesoproteins (green) and protons attached to C(δ) and C(ϵ) of the coordinating histidine (red), with the parameters collected in Table 1.

HYSCORE Signals Due to Weakly Coupled Nitrogens.

In the X-band HYSCORE spectrum of Figure 2, there is a dense region of partially overlapping correlations at frequencies below 5 MHz. They are centered around $2\nu_N$ ($I = 1$) and on ν_C ($I = 1/2$), showing signals of nuclei in the heme pocket that have not been observed previously with other EPR techniques for HS heme centers. The signals vanish in the X-band HYSCORE spectra on going to B_0 fields lower than 300 mT. However, the Q-band HYSCORE spectra at observer positions in the range of $g^{\text{eff}} = 4-6$ are very rich

in the low frequency region of the (+, +) quadrant (Figure 5B and C show two of these spectra). As a result of the increase in the Zeeman interaction, the ^{13}C contributions are well-separated from the ^{14}N signals in the Q-band HYSCORE spectra, which simplifies the spectral interpretation. It should be noted that these interactions could not be detected using Q-band Mims or Davies ENDOR.

The most intense correlations of the X-band HYSCORE spectrum of Figure 5A are at (2.9, 2.1) MHz, for which the average frequency lies approximately 0.5 MHz above $2\nu_N$.

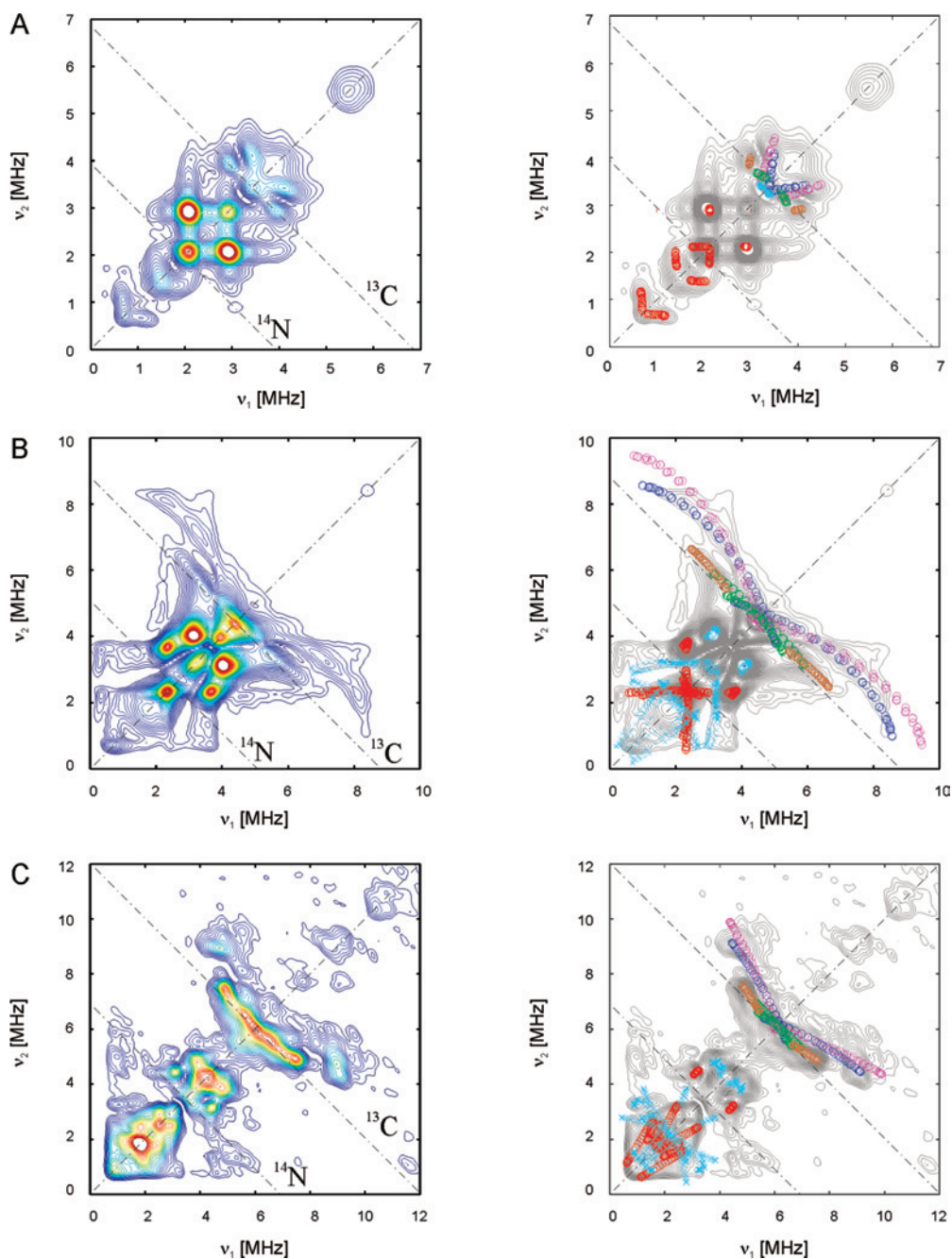


Figure 5. HYSCORE spectra showing the contributions of the weakly coupled ^{14}N and ^{13}C . (A) X-band HYSCORE spectrum $B_0 = 320$ mT, $\tau = 128$ ns. (B) Q-band HYSCORE spectrum $B_0 = 412$ mT ($g = g_{\perp}^{\text{eff}}$), $\tau = 80$ ns. (C) Q-band HYSCORE spectrum $B_0 = 562$ mT, $\tau = 80$ ns. The experimental spectra are shown alone on the left and together with the superimposed frequency calculations on the right. The red circles correspond to the calculated nuclear frequencies for the N_{δ} of the coordinating His, and the cyan crosses correspond to the ones calculated for the N_{ϵ} of the distal His. The parameters used for the calculations are collected in Table 2. Only the relevant correlations are shown. The pattern of nuclear frequencies calculated for ^{13}C are displayed in green for the mesocarbons and brown for β -pyrrole carbons. α -Pyrrole carbons are displayed in blue (option 1) and magenta (option 2).

Table 2. ^{14}N Hyperfine and Nuclear Quadrupole Parameters Used for the Calculation of the Nuclear-Frequency HYSCORE Patterns of the Detected Remote Nitrogens in Figure 5^a

	A_x	A_y	A_z	γ	β	α	Q_x	Q_y	Q_z	γ	β	α
N_δ (F8, His93)	0.3	0.3	0.5	0	0	11	0.69	-0.85	0.16	0	-36	11
N_ϵ (E7, His64)	-0.27	-0.27	-0.07	0	24	45	0.65	0.9	-1.55	0	55	0

^a The principal values of the tensors are expressed in MHz, and their Euler angles with respect to the principal axes of the \mathbf{g} tensor are given in degrees.

Table 3. ^{13}C Hyperfine Parameters Used for the Calculation of the Nuclear-Frequency HYSCORE Patterns of the Pyrrole and Meso Carbons (^{13}C) in Isotopic Natural Abundance in Figure 5^a

	r (Å)	ϕ (deg)	T	A_{iso}	A_z^*	A_y^*	A_x^*	β (deg)	γ (deg)
pyrrole α (1)	3.04	22	0.71	0.8	0.7	-0.8	0.1	90	54
pyrrole α (2)	3.04	22	0.71	1.2	0.9	-0.9	0.0	90	54
pyrrole β	4.27	10	0.26	1.0	0.2	-0.1	-0.1	0	
meso	3.4	45	0.50	-0.07	0	0	0		

^a A_{iso} is the isotropic hyperfine value as obtained from the simulations. T dipolar (in megahertz) is calculated by a point-dipole approximation, using the distance $r(\text{Fe}-\text{C})$ as obtained by X-ray data and an angle $\theta = 90^\circ$; ϕ is the angle between r and the coordinating N direction. A_x^* , A_y^* , and A_z^* (also in megahertz) were obtained from the simulations and refer to the principal values of an extra anisotropic contribution. The Euler angles of this contribution are $\alpha = 0^\circ$, β , and γ . Pyrrole α (1) and α (2) indicate two different possibilities. Pyrrole α (2) is an option using A_{iso} from the NMR study,⁹ see the text.

These peaks can be assigned to double-quantum (dq) features of a weakly coupled nitrogen. Similarly, the correlation peaks at (2.3, 3.7) MHz in the Q-band HYSCORE spectrum (Figure 5B) can be assigned to the dq nuclear frequencies of this nitrogen. The correlation patterns were simulated using the parameters reported in Table 2 (simulations shown in Figure 5).

The hyperfine values deviate strongly from the ones of the directly coordinated histidine and heme nitrogens.^{7,14} The nuclear quadrupole parameter that was obtained ($K = 0.4$ MHz) is typical for protonated nitrogens of imidazoles, and hence, the signals can be assigned to the remote nitrogen, N_δ , of the F8His.³³ Confirming this assignment is the fact that these correlation peaks were also found in the X-band HYSCORE spectrum of E7Q-neuroglobin recorded at a field position corresponding to $g_{\parallel}^{\text{eff}}$ ¹⁵ but were not visible in the equivalent spectrum of a model complex of cyt P450 for which the proximal axial ligand is a sulfonyl group.³⁴

In the Q-band HYSCORE spectra (Figure 5B and C), the most intense cross peaks stem from yet another nitrogen nucleus. The peaks are centered at a frequency about 1 MHz higher than $2\nu_{\text{N}}$, indicating that this nucleus has a larger nuclear quadrupole value. The N_ϵ of the distal unbound His is a likely candidate (Figure 1). This nucleus is expected to have a small hyperfine coupling and could therefore contribute in this region of the spectrum. In view of the large distance between this N and the Fe (0.44 nm), a point-dipole approximation was used to first estimate the hyperfine tensor of this nucleus, $T = 0.07$ MHz. To optimally fit the spectra, an isotropic contribution $A_{\text{iso}} = -0.2$ MHz had to be added. From the optimal spectral simulations (Figure 5), a value of $K = 0.77$ MHz is obtained. This nuclear quadrupole value is close to the one found for nonprotonated nitrogens in an imidazole ring,^{33,35} which confirms our assignment.

The simulated positions of the HYSCORE correlation ridges are shown in Figure 5 in red (N_δ) and cyan (N_ϵ).

^{13}C HYSCORE Signals. In the HYSCORE spectra of Figure 5, the appearance of the correlation peaks in the region around ν_{C} indicates that hyperfine interactions with ^{13}C nuclei in natural abundance (1.1%) are detected. To find out whether

the ^{13}C signals are due to heme or protein carbons, analogous X-band HYSCORE experiments were performed in a water/dimethylsulfoxide (1:1) hemin solution. As all of the signals were also present in the hemin complex (see the Supporting Information), they were assigned to heme carbons. Equivalent Q-band HYSCORE experiments of the hemin complex could not be performed due to the shorter relaxation times. These imply that the experiments need to be performed at lower temperatures for the hemin case than for aquometMb, which was technically not possible in the Q-band EPR setup. Note that signals around ν_{C} were visible in the HYSCORE spectra of a model complex of cyt P450 but were not interpreted as such.³⁴

To assign the signals to a particular kind of heme carbon, the nuclei in the closest vicinity of the iron atom were considered, that is, pyrrole α , pyrrole β , and mesocarbons in the porphyrin ring. In a first approach, a point-dipole hyperfine interaction was used to calculate the orientation dependence of the ^{13}C signals, considering 100% spin density on the Fe atom ($f = 1$). The Fe-C distances and orientations with respect to the \mathbf{g} -tensor frame were taken from the X-ray structure of the protein.²⁹⁻³¹ On this basis, the correlations could be assigned to the different ^{13}C nuclei, and the hyperfine parameters were further refined until a satisfactory simulation of the nuclear frequencies was obtained (see Figure 5). The parameters are reported in Table 3. It has to be noted that, for the pyrrole α carbons, the anisotropic contribution deviates substantially from the one calculated on the basis of a simple point-dipole approximation.

Discussion

The combination of HYSCORE experiments at different frequencies has allowed for the analysis of the hyperfine

- (31) Tanako, T. *J. Mol. Biol.* **1977**, *110*, 537.
- (32) Schweiger, A.; Jeschke, G. *Principles of Pulse Electron Paramagnetic Resonance*; Oxford University Press: Oxford, U.K., 2001; p 214.
- (33) Hunt, M. J.; Mackay, A. L.; Edmons, D. T. *Chem. Phys. Lett.* **1975**, *34*, 473.
- (34) Bachmann, R.; Schweiger, A.; Aissaoui, H.; Woggon, W. D. In *Joint 29th AMPERE - 13th ISMAR International Conference*, TU Berlin, 1998; Ziessow, D., Lubitz, W., Lendzian, F., Eds.; TU Berlin: Berlin, 1998; pp 822.
- (35) Ashby, C. I. H.; Cheng, C. P.; Brown, T. L. *J. Am. Chem. Soc.* **1978**, *100*, 6057.

parameters of numerous magnetic nuclei in the active site of aquometMb.

Analysis of the Proton Hyperfine Couplings. The HYSORE spectra collected in Figures 3 and 4 provide the most extensive information available at the moment about the hyperfine tensor of the protons closest to the heme iron. The HYSORE cross peaks assigned to the mesoprotons can be traced in our data for a wide variety of orientations of the magnetic field. The nuclear-frequency calculations shown in the figures have all been performed with the parameters collected in Table 1. The used A_{iso} value of the mesoprotons (0.06 MHz) was derived from the chemical shifts in the liquid-state NMR study of metmyoglobin at room temperature⁹ and is perfectly compatible with the current data. The anisotropic part of the hyperfine interaction was calculated using the point-dipole approximation (eq 3) with $r = 0.445$ nm and assuming that the mesoprotons lie in the heme plane.⁷ It has been suggested that a better approach to compute the anisotropic contribution of the hyperfine interaction would be to consider the sum of interactions of a nuclear point dipole and several electron point dipoles weighted according to the spin population in the different atoms of the heme site.³⁶ We have performed such kind of calculations to fit our data but were confronted with the following problems. First, this type of calculation requires an exact knowledge of the spin distribution within the site. In the literature, different data about the spin distribution in HS heme systems have been reported, with the spin population in the iron ranging from 63%³⁷ to 68%⁷ to 80–83%.¹³ Second, for distances shorter than 0.25 nm, the point-dipole approximation is no longer valid. Moreover, in general, this approach did not lead to a better fit than the point-dipole approximation. For the sake of simplicity, we therefore decided to limit ourselves to the point-dipole approximation, leaving a multiplicative adjustable parameter (f in eq 3 and Table 1) that would account not only for spin densities lower than 1 in the iron but also possible effects due to considerable spin populations on other atoms. The nuclear frequency patterns calculated in this way reproduce very satisfactorily the position and shape of the mesoproton correlation ridges observed in the experimental spectra. The best agreement for the mesoprotons was found for $f = 0.9$. Although no mesoproton signals can be distinguished in the HYSORE spectra taken at an observer position near $g = g_z^{\text{eff}}$, our calculations are compatible with the nuclear frequencies at this position obtained in an earlier CW-ENDOR study.⁴

For the heme methyl protons, similar calculations using the point-dipolar approximation and the value of A_{iso} determined by NMR (0.24 MHz⁹) yield patterns compatible with signals in the spectra of Figure 3 (not shown). Nevertheless, the high degree of superposition of these patterns with the ones of the mesoprotons makes it impossible to substantiate that we are actually detecting these kinds of protons.

For the protons attached to the histidine carbons C(ϵ) and C(δ), no information on A_{iso} could so far be obtained using NMR. The analysis of our data, following the above methodology, allows a fairly detailed determination of the hyperfine tensor, which is again compatible with the calculations made using the point-dipole approximation and an isotropic contribution that was evaluated to be $A_{\text{iso}} = +0.2 \pm 0.2$ MHz. The positive sign of the isotropic contribution means that the spin transfer to these nuclei is dominated by the σ -bonding interaction with the semiooccupied d_{z^2} orbital of the iron. In low-spin bis-imidazole complexes values of A_{iso} of -0.93 and -0.27 MHz were found for these protons³⁸ where this mechanism of spin delocalization is not present because the d_{z^2} iron orbital is empty.

Maybe the most unexpected finding in the analysis of the proton signals is the resolution of two different water protons. They are not resolved in the spectra or the simulations taken at an observer position $g = g_z^{\text{eff}}$, but at other magnetic field positions, two separated ridges can be distinguished. The position and shape of these lines are well-reproduced with the parameters collected in Table 1 for all of the spectra. The values of the distances and angles used for the calculations are very close to those found in the crystal structures of metmyoglobin. Nevertheless, in the case of the water protons, which are attached to the axial oxygen atom carrying some spin density (4.6%¹⁴), the validity of the point-dipole approximation is at the limit, and consequently, the values of the geometrical parameters given in Table 1 cannot be taken to be exact. However, the fact that the anisotropic contribution of the hyperfine for both protons is different suggests an asymmetric spatial arrangement of the water molecule with respect to the iron. This arrangement is most probably forced by the hydrogen bond existing between the axial water molecule and N(ϵ) of His 64, which is reflected in the N(ϵ) His64 nuclear quadrupole values (see below).

Identification of the HYSORE Contributions of the Remote Nitrogens. Two distinct remote nitrogens have been detected. Table 2 collects the parameters used for the calculated nuclear-frequency patterns shown in Figure 5.

For the N_{δ} nucleus of the proximal histidine, an axial hyperfine tensor was found with the distinguished axis perpendicular to the heme plane (the Euler angle α was set to 11° to reflect the arrangement of the histidine plane,⁷ but it had no effect on the calculations as the hyperfine matrix is (within the experimental error) axial in the heme plane). The hyperfine interaction determined for the directly coordinated nitrogen of the same histidine residue (N_{ϵ}) is quasi axial with principal values that are about 25 times larger. The ratio between the hyperfine of the coordinating and the remote nitrogens of the His has been reported to be approximately 20 for copper-coordinated histidines.³⁹ This supports our assignment and shows that approximately the same ratio is valid for histidine residues coordinated to iron.

(37) Mallick, M. K.; Chang, J. C.; Das, T. P. *J. Chem. Phys.* **1978**, *68*, 1462.

(38) Satterlee, J. D.; Lamar, G. N. *J. Am. Chem. Soc.* **1976**, *98*, 2804.

(39) Coremans, J. W.; Poluektov, O. G.; Groenen, E. J. J.; Canters, G. W.; Nar, H.; Messerschmidt, A. *J. Am. Chem. Soc.* **1996**, *118*, 12141.

(36) Mun, S. K.; Mallick, M. K.; Mishra, S.; Chang, J. C.; Das, T. P. *J. Am. Chem. Soc.* **1981**, *103*, 5024.

The orientation of the nuclear quadrupole tensor was used as reported in the literature for other metal–histidine complexes³⁵ and the spatial arrangement of the histidine according to the X-ray structure of aquometMb.^{29,31}

The spectral features assigned to N_ϵ of the distal His64 (E7) are well reproduced with a hyperfine tensor calculated using the pure point-dipole approximation (eq 3 with $f = 1$) with the values for the distance N–Fe (4.4 Å) and the θ angle taken from the protein structure (24°) and an isotropic component, $A_{\text{iso}} = -0.2$ MHz. The nuclear quadrupole tensor obtained from our data, with values $e^2qQ/h = 3.1$ MHz and $\eta = 0.16$, is close to the one reported for the hydrogen-bonded N_ϵ of histidine in different imidazole compounds.^{33,40,41} The fact that the dq cross peaks of N_ϵ of the distal His64 (E7) can be readily observed using Q-band HYSCORE (Figure 5B) offers a means of detecting the stabilization of water by distal histidines in other, less explored aquometoglobins.

Analysis of the Spin-Hamiltonian Parameters of the Heme Carbons. From our experimental results, it is clear that we can detect the interaction of the unpaired electron with different types of ^{13}C nuclei in the active site of the protein. Moreover, from the X-band HYSCORE measurements done in a hemin solution, it seems that all of them stem from the porphyrin ring.

Following the pattern-calculation procedure, we could assign the spectral features appearing in the outer part of the ν_C antidiagonal in Figure 5 (colored in brown in the simulation) to the β -pyrrole carbons. Initially, the nuclear-frequency calculations were performed using the geometrical data collected in Table 3 ($T = 0.26$ MHz) and an isotropic contribution, $A_{\text{iso}} = 1.0$ MHz, in agreement with the liquid NMR data of metmyoglobin at room temperature ($\delta(C_{\beta\text{-pyrrole}}) = 1200$ ppm¹²). However, in order to better reproduce the experimental ridges, a small additional component needed to be added (A^*). Table 3 shows the individual contributions to the hyperfine matrix, whereby the full hyperfine matrices are given in the Supporting Information. The additional axial contribution (A^*) with the distinguished axis along the heme normal is probably due to a small spin population in the p_z orbital of this atom (π orbital of the porphyrin ring) that was calculated to be 0.0053.^{14,42}

The mesocarbon features were calculated with the same approach using a small and negative value for $A_{\text{iso}} = -0.07$ MHz as was obtained from NMR (see green pattern in Figure 5). Consequently, the central features on the ν_C antidiagonal can be assigned to the mesocarbons. These features partially overlap with the ones from the β -pyrrole carbons and are not optimally resolved.

The HYSCORE spectra measured at X- and Q-band frequencies show correlations clearly shifted away from the ν_C antidiagonal, which proved to be associated with a porphyrin carbon (hemin solution experiments). The strong curvature of the ridges indicates that the hyperfine coupling is strongly anisotropic. The α -pyrrole carbons are the ones

closest to the Fe^{3+} . They are directly bound to the coordinating heme nitrogens, and therefore, their hyperfine interaction is expected to be the largest. In the Q-band HYSCORE spectrum taken at g_\perp^{eff} (Figure 5B), the observed ridges are quite long, indicating a very anisotropic hyperfine interaction in the heme plane. This fact supports the hypothesis that the nucleus is located in the heme plane rather than close to the normal, and we therefore assign these ridges to the α -pyrrole carbons.

The first simulation approach taking into account only the point-dipole approximation and the isotropic contribution obtained from NMR ($A_{\text{iso}} = 1.2$ MHz) produced highly anisotropic lines but did not yield satisfactory agreement (see the Supporting Information). The experimental shape seemed to correspond to a more anisotropic interaction. Considering that the α -pyrrole carbon is attached to the coordinating nitrogen (bond distance 1.4 Å) and this nitrogen bears considerable spin density,^{7,14} the hyperfine coupling of the α -pyrrole carbon cannot be appropriately evaluated by the point-dipole approximation. Moreover, it is expected that the spin density in the iron-binding orbital of the nitrogen polarizes the N–C binding orbital, generating also an anisotropic hyperfine interaction with the ^{13}C nucleus (and probably of the opposite sign to the delocalized spin density on the nitrogen). To take into account these interactions, we considered an additional hyperfine contribution with one of the principal axes oriented along the N–C direction (54° with respect to the Fe–N direction of the same pyrrole ring), and one along the heme normal. The principal values of this contribution were adjusted to fit the experimental spectra. The best fit (shown in blue in Figure 5) is obtained using the parameters listed as option 1 in Table 3. Hereby, the A_{iso} value differs from the one found by NMR, which is equal to 1.2 MHz.¹² When A_{iso} is fixed to 1.2 MHz, the outer part of the ridge in Figure 5B cannot be accurately fitted. The best fit with this constraint is shown in magenta in Figure 5 and labeled as option 2 for the α -pyrrole carbons in Table 3. However, this option requires assignment of the outer part of the ridge to another carbon nucleus. In both options, the additional hyperfine contribution is not axial with respect to the N–C bond axis. This indicates that there is, besides a σ -bond contribution, also a certain amount of spin density in the p_z orbital of the carbon as can be expected for a strong π system. The contribution of this spin density is also expected to be axial in the heme normal direction. If we define the parameters T_σ and T_π to characterize the in-plane and out-of-plane axial contributions, one should expect to have $2T_\sigma - T_\pi$ along the N–C direction (z'), $2T_\pi - T_\sigma$ along the heme normal (x'), and $-T_\sigma - T_\pi$ along the third direction (y'). With the hyperfine matrix obtained from the pattern calculations, a value of $T_\pi = 0.3$ MHz (both options) and $T_\sigma = 0.5$ MHz (option 1) or 0.6 MHz (option 2) can be obtained. These values of the anisotropic hyperfine translate into a spin density in the N– ^{13}C σ

(40) MacDowell, C. A.; Naito, A.; Sastry, D. L.; Takegoshi, K. *J. Magn. Reson.* **1986**, *69*, 283.

(41) Palmer, M. H.; Scott, F. E.; Smith, J. A. S. *Chem. Phys.* **1983**, *74*, 9.

(42) Fitzpatrick, J. A. J.; Manby, F. R.; Western, C. M. *J. Chem. Phys.* **2005**, *122*.

orbital of 0.027–0.032 and a spin density of 0.016 in the π orbital.^{14,42}

The π spin densities in the α - and β -pyrrole carbons are on the same order of magnitude as the ones calculated using DFT for the six-coordinated high-spin iron(III)–porphyrin complex $\text{FeP}(\text{H}_2\text{O})_2$.¹³ However, we obtain about a 3 times higher spin density in the $^{\alpha}\text{C}$ than in the $^{\beta}\text{C}$, while exactly the opposite is found for the theoretical model, $\text{FeP}(\text{H}_2\text{O})_2$. However, the latter system has D_{2h} symmetry. In the aquometmyoglobin case, the asymmetry of the axial ligands reduces the point group of the site to D_{2d} . For this symmetry, mixtures between the semioccupied iron orbital d_{xy} and the occupied π frontier orbital of the porphyrin b_1 (a_{1u} when the symmetry is D_{4h}) are allowed, while they are forbidden in the case of D_{2h} symmetry.¹³ This frontier orbital has more π spin population on $^{\alpha}\text{C}$ than on $^{\beta}\text{C}$, so our results could be indicating that the mechanism of spin delocalization is produced via this mixing rather than via the interaction between the iron orbitals d_{xz} and d_{yz} with either the occupied or the empty e porphyrin frontier orbitals, which have more π spin population on $^{\beta}\text{C}$.

Conclusions

Using multifrequency HYSCORE spectroscopy, the EPR parameters of weakly coupled nuclei in the active center of the high-spin aquometmyoglobin could be determined. The HYSCORE spectra revealed the hyperfine interactions of the protons of the proximal histidine ligand, of the mesoprotons, and of two different protons of the distal water ligand. The HYSCORE signals of the remote N_δ of the proximal histidine and of N_ϵ of the distal histidine were detected and interpreted. The possibility to detect the hyperfine coupling of the latter

nitrogen and the slight differences between the hyperfine interactions of the two water protons opens the way to investigate stabilization of the axial water by the distal histidine in other aquometglobins. Furthermore, correlation patterns assigned to ^{13}C nuclei, present in aquometmyoglobin in isotopically natural abundance (1.1%), could be observed. This allowed obtaining the hyperfine interactions of the carbons in the porphyrin ring. All of these interactions were revealed at several magnetic-field settings, therefore allowing the determination of all the principal values of the nuclear interactions. The ^{13}C data complete the information that could earlier be revealed by paramagnetic NMR (revealing only the isotropic part of hyperfine coupling). The current work offers a unique experimental data set that can be used to verify the quality of future quantum-chemical computations of the heme pocket of high-spin ferric globins.

Acknowledgment. This paper is dedicated to the memory of Prof. Arthur Schweiger, who supported this project at its early stage. Financial support was given by the Swiss National Science Foundation, the Italian Ministero dell'Istruzione, dell'Università e della Ricerca, the Fund of Scientific Research-Flanders, and COST action P15.

Supporting Information Available: Simulation of the deuterium signal present in the X-band HYSCORE spectrum taken at g_{\parallel} . X-band HYSCORE spectrum of heme in solution taken at an observer position near g_{\parallel} . Full hyperfine matrices of the different observed ^{13}C couplings. Q-band spectrum at $g = g_{\perp}^{\text{eff}}$ with the calculated pattern for α -pyrrole carbons taking into account only an isotropic and point-dipole hyperfine contributions. This material is available free of charge via the Internet at <http://pubs.acs.org>.

IC8016886